

Inverse Optimization Techniques for Targeted Self-Assembly

Salvatore Torquato*

*Department of Chemistry, Princeton Center for Theoretical Science,
Princeton Institute for the Science and Technology of Materials,
and Program in Applied and Computational Mathematics,
Princeton University, Princeton, New Jersey 08544, USA;*

*and School of Natural Sciences, Institute for Advanced Study, Princeton, New Jersey, 08540, USA
(Dated: February 11, 2022)*

This article reviews recent inverse statistical-mechanical methodologies that we have devised to optimize interaction potentials in soft matter systems that correspond to stable “target” structures. We are interested in finding the interaction potential, not necessarily pairwise additive or spherically symmetric, that stabilizes a targeted many-body system by generally incorporating complete configurational information. Unlike previous work, our primary interest is in the possible many-body structures that may be generated, some of which may include interesting but known structures, while others may represent entirely new structural motifs. Soft matter systems, such as colloids and polymers, offer a versatile means of realizing the optimized interactions. It is shown that these inverse approaches hold great promise for controlling self-assembly to a degree that surpasses the less-than-optimal path that nature has provided. Indeed, we envision being able to “tailor” potentials that produce varying degrees of disorder, thus extending the traditional idea of self-assembly to incorporate both amorphous and crystalline structures as well as quasicrystals. The notion of tailoring potentials that correspond to targeted structures is motivated by the rich fundamental statistical-mechanical issues and questions offered by this fascinating inverse problem as well as our recent ability to identify structures that have optimal bulk properties or desirable performance characteristics. Recent results have already led to a deeper basic understanding of the mathematical relationship between the collective structural behavior of many-body systems and their interactions, as well as optimized potentials that enable self-assembly of ordered and disordered particle configurations with novel structural and bulk properties.

I. INTRODUCTION

The term “self-assembly” typically describes processes in which entities (atoms, molecules, aggregates of molecules, etc.) spontaneously arrange themselves into a larger ordered and functioning structure. Biology offers wonderful examples, including the spontaneous formation of the DNA double helix from two complementary oligonucleotide chains, the formation of lipid bilayers to produce membranes, and the folding of proteins into a biologically active state.

On the synthetic side, molecular self-assembly is a potentially powerful method to fabricate nanostructures as an alternative to nanolithography. For example, it has been demonstrated that intricate two-dimensional structures can emerge by the placement of organic molecules onto inorganic surfaces.¹ Block copolymers can self-assemble into ordered arrays that have possible use as photonic band-gap materials.² Self-assembly based on contact electrification seems to be a powerful means to organize macroscopic dielectric particles of various shapes into extended, ordered structures.³ Highly robust self-assembly of unique, small clusters of microspheres that can themselves be used for self-assembly of more complex architectures has been demonstrated.⁴ It has been shown that gold nanowires can be assembled by functionalizing nanoparticles with organic molecules.⁵ DNA-mediated assembly of micrometer-size polystyrene particles in solution could enable one to build complex structures starting from a mesoscale template or seed fol-

lowed by self-assembly.⁶ These examples offer glimpses into the materials science of the future – devising building blocks with specific interactions that can self-organize on a larger set of length scales.

This is an emerging field with a wealth of experimental data that has been supported theoretically and computationally using the “forward” approach of statistical mechanics.^{7,8,9,10,11,12,13,14,15,16} Such an approach has generated a long and insightful tradition. The forward approach identifies a known material system that possesses scientific and/or technological interest, creates a manageable approximation to the interparticle interactions that operate in that material, and exploits simulation and analytical methods to predict non-obvious details concerning structural, thermodynamic and kinetic features of the system.

In the last several years, *inverse* statistical-mechanical methods have been devised that find optimized interactions that most robustly and spontaneously lead to a targeted many-particle configuration of the system for a wide range of conditions.^{17,18,19,20,21,22,23,24,25,26,27} This article reviews these nascent developments as well as other closely related inverse realizability problems that we have introduced,^{28,29,30,31,32,33,34,35,36,37} all of which are solved using various optimization techniques.

Results produced by these inverse approaches have already led to a deeper fundamental understanding of the mathematical relationship between the collective structural behavior of many-body systems and the interactions: a basic problem in materials science and con-

densified matter theory. As will be shown, such methodologies hold great promise to control self-assembly in many-particle systems to a degree that surpasses the less-than-optimal path that nature has provided. Indeed, employing such inverse optimization methods, we envision being able to “tailor” potentials that produce varying degrees of disorder, thus extending the traditional idea of self-assembly to incorporate both amorphous and crystalline structures as well as quasicrystals.

Output from these optimization techniques could then be applied to create *de novo* colloidal particles or polymer systems with interactions that yield these structures at the nanoscopic and microscopic length scales. Thus, this work has important implications for the future synthesis of novel materials.

Colloidal particles suspended in solution provide an ideal experimental testbed to realize the optimized potentials, since both repulsive and attractive interactions can be tuned (*e.g.*, via particle surface modification or the addition of electrolytes).^{4,6,14,38,39,40,41,42} and therefore offer a panoply of *possible* potentials that far extends the range offered by molecular systems. Effective pair interactions in colloids can contain hard-core, charge dispersion (van der Waals), dipole-dipole (electric- or magnetic-field induced⁴²), screened-Coulombic (Yukawa), and short-ranged attractive depletion contributions. Polymer systems also offer a versatile means of realizing optimized soft interactions.^{11,43}

The idea of *tailoring* potentials to generate targeted structures is motivated by the rich array of fundamental issues and questions offered by this fascinating inverse statistical-mechanical problem as well as our recent ability to identify the structures that have optimal bulk properties or desirable performance characteristics. The latter includes novel crystal^{44,45,46} and quasicrystal^{25,47} structures for photonic band-gap applications, materials with negative or vanishing thermal expansion coefficients,^{48,49,50} materials with negative Poisson ratios,^{26,51,52,53,54,55,56} materials with optimal or novel transport and mechanical properties,^{57,58,59,60,61,62,63} mesoporous solids for applications in catalysis, separations, sensors and electronics,^{64,65} and systems characterized by entropically driven inverse freezing,^{66,67} to mention a few examples.

The recent inverse techniques that are reviewed here differ from so-called “reverse” Monte Carlo methods^{68,69,70,71} in several important respects. The latter techniques are concerned almost invariably with obtaining a spherically symmetric pair potential from an experimentally observed structure factor (as measured from scattering experiments) or real-space pair correlation function usually for stable liquid phases or glassy states of matter. By contrast, our interest is in finding the interaction potential, not necessarily pairwise additive or spherically symmetric, that optimally stabilizes a targeted many-body system, which may be a crystal, disordered or quasicrystal structure, by incorporating structural information that is not limited to the pair

correlation function and generally accounts for complete configurational information. Unlike previous work, our primary interest is in the possible many-body structures that may be generated, some of which may include interesting but known structures, while others may represent entirely new structural motifs. Moreover, the inverse methods described here can be employed to find targeted structures for metastable states as well as nonequilibrium configurations.

In Section II, we define essential terms and briefly review basic concepts that are germane to the remainder of the article. Section III describes inverse optimization methods for self-assembly of crystal ground states. In Section IV, we discuss recent applications of these methods that yield unusual crystal ground states with optimized, nondirectional interactions, including low-coordinated structures, chain-like arrays, and lattices of clusters. Section V describes and applies inverse optimization methods for self-assembly of disordered ground states. In Section VI, new duality relations for classical ground states are reviewed and applied to some cases examined in the previous sections. Section VII discusses the pair-correlation-function realizability problem and inverse optimization procedures to construct configurations with a given pair correlation function. In Section VIII, we discuss inverse optimization methods to optimize interactions for targeted bulk properties and specific applications. Finally, in Section IX, we suggest problems for future work and close with concluding remarks.

II. BASIC DEFINITIONS AND CONCEPTS

We consider a configuration of N identical interacting particles with coordinates $\mathbf{r}^N \equiv \mathbf{r}_1, \mathbf{r}_2, \dots, \mathbf{r}_N$ in a region of volume V in d -dimensional Euclidean space \mathbb{R}^d . The coordinate \mathbf{r}_i of the i th particle generally embodies both its center-of-mass position and orientation as well as conformation if required. In the absence of an external field, the classical N -body potential Φ_N can be decomposed into 2-body terms, 3-body etc., as follows:

$$\Phi_N(\mathbf{r}^N) = \sum_{i < j}^N \varphi_2(\mathbf{r}_i, \mathbf{r}_j) + \sum_{i < j < k}^N \varphi_3(\mathbf{r}_i, \mathbf{r}_j, \mathbf{r}_k) + \dots \quad (2.1)$$

Here φ_n is the intrinsic n -body potential in *excess* to the contributions from $\varphi_2, \varphi_3, \dots, \varphi_{n-1}$.

A given many-body structure is specified by the local density $\rho(\mathbf{r})$, which can be expressed in terms of the particle coordinates as follows:

$$\rho(\mathbf{r}) = \sum_{i=1}^N \delta(\mathbf{r} - \mathbf{r}_i), \quad (2.2)$$

where $\delta(\mathbf{r})$ is the d -dimensional Dirac delta function. The N particle coordinates \mathbf{r}^N are statistically characterized by the ensemble (equilibrium or not) under consideration. The ensemble average of n products of the local

densities at n different positions yields the standard n -particle correlation functions.³⁵ For statistically homogeneous systems in a volume V , these correlation functions are defined so that $\rho^n g_n(\mathbf{r}^n)$ is proportional to the probability density for simultaneously finding n particles at locations $\mathbf{r}^n \equiv \mathbf{r}_1, \mathbf{r}_2, \dots, \mathbf{r}_n$ within the system⁷, where $\rho = N/V$ is the number density. With this convention, each g_n approaches unity when all particle positions become widely separated within V . Statistical homogeneity implies that g_n is translationally invariant and therefore only depends on the relative displacements of the positions with respect to some arbitrarily chosen origin of the system, *i.e.*,

$$g_n = g_n(\mathbf{r}_{12}, \mathbf{r}_{13}, \dots, \mathbf{r}_{1n}), \quad (2.3)$$

where $\mathbf{r}_{ij} = \mathbf{r}_j - \mathbf{r}_i$.

The *pair correlation function* $g_2(\mathbf{r})$ is the one of primary interest in this review. If the system is also rotationally invariant (statistically isotropic), then g_2 depends on the radial distance $r \equiv |\mathbf{r}|$ only, *i.e.*, $g_2(\mathbf{r}) = g_2(r)$. It is important to introduce the *total correlation function* $h(\mathbf{r}) \equiv g_2(\mathbf{r}) - 1$, which, for a *disordered* system, decays to zero for large $|\mathbf{r}|$ sufficiently rapidly.³⁵

Such pair statistics can be inferred from radiation scattering experiments via the structure factor.⁷ The *structure factor* $S(\mathbf{k})$, for an N -particle system is related to the *collective density* variable

$$\tilde{\rho}(\mathbf{k}) = \sum_{j=1}^N \exp(i\mathbf{k} \cdot \mathbf{r}_j), \quad (2.4)$$

via the expression

$$S(\mathbf{k}) = \frac{|\tilde{\rho}(\mathbf{k})|^2}{N}, \quad (2.5)$$

where $\tilde{\rho}(\mathbf{k})$ is the Fourier transform of $\rho(\mathbf{r})$, defined by (2.2), and $i = \sqrt{-1}$. Since the structure factor is proportional to the intensity of the scattered radiation, it is a nonnegative quantity for all \mathbf{k} , *i.e.*,

$$S(\mathbf{k}) \geq 0 \quad \text{for all } \mathbf{k}. \quad (2.6)$$

This also mathematically follows from the nonnegative form (2.5). In the thermodynamic limit ($N \rightarrow \infty$, $V \rightarrow \infty$ such that ρ is a fixed positive constant), the ensemble-averaged structure factor (omitting forward scattering) is defined by

$$S(\mathbf{k}) = 1 + \rho \tilde{h}(\mathbf{k}), \quad (2.7)$$

where $\tilde{h}(\mathbf{k})$ is the Fourier transform of the total correlation function $h(\mathbf{r})$.

The structure factor $S(\mathbf{k})$ provides a measure of the density fluctuations at a particular wave vector \mathbf{k} . To see this important property quantitatively, consider the point pattern defined by the centers of particles in a many-body system at number density ρ . Let $\sigma^2(R)$ denote the *number variance* of points contained within a

d -dimensional spherical window of radius R in \mathbb{R}^d . It can be shown⁷² that the number variance has the following real-space and Fourier-space representations:

$$\begin{aligned} \sigma^2(R) &= \rho v_1(R) \left[1 + \rho \int_{\mathbb{R}^d} h(\mathbf{r}) \alpha(r; R) d\mathbf{r} \right] \\ &= \rho v_1(R) \left[\frac{1}{(2\pi)^d} \int_{\mathbb{R}^d} S(\mathbf{k}) \tilde{\alpha}(\mathbf{k}; R) d\mathbf{k} \right], \end{aligned} \quad (2.8)$$

where $v_1(R) = \pi^{d/2} R^d / \Gamma(1 + d/2)$ is the volume of the spherical window of radius R , $\alpha(r; R)$ is *scaled intersection volume*, equal to the volume common to two spherical windows of radius R whose centers are separated by a distance r divided by $v_1(R)$, and $\tilde{\alpha}(\mathbf{k}; R)$ is the corresponding Fourier transform of $\alpha(r; R)$. The scaled intersection volume $\alpha(r; R)$ and its Fourier transform $\tilde{\alpha}(\mathbf{k}; R)$ can be expressed explicitly in any dimension d .^{35,72} Thus, we see that the structure factor is directly related to the number variance at different wavelengths or, equivalently, for different window radii. In the limit of an infinitely large window, the relation above yields

$$\lim_{R \rightarrow \infty} \frac{\sigma^2(R)}{\rho v_1(R)} = S(\mathbf{k} = \mathbf{0}) = 1 + \rho \int_{\mathbb{R}^d} h(\mathbf{r}) d\mathbf{r}. \quad (2.9)$$

Formula (2.9) applies whether the system is in equilibrium or not. In the special case of an equilibrium system, it is well known that infinite-wavelength density fluctuations, as expressed by (2.9), are proportional to the isothermal compressibility of the system.⁷

For large R , it has been proved that $\sigma^2(R)$ cannot grow more slowly than γR^{d-1} or window surface area, where γ is a positive constant.⁷³ We note that point processes (translationally invariant or not) for which $\sigma^2(R)$ grows more slowly than R^d (*i.e.*, window volume) for large R are examples of *hyperuniform* (or superhomogeneous) point patterns.^{72,74} Hyperuniformity implies that the structure factor $S(\mathbf{k})$ has the following small \mathbf{k} behavior:

$$\lim_{\mathbf{k} \rightarrow \mathbf{0}} S(\mathbf{k}) = 0. \quad (2.10)$$

This classification includes all crystal structures,⁷² point patterns associated with periodic and certain aperiodic tilings of space,^{72,74,75,76} one-component plasmas,^{72,74} distribution of matter in the early Universe,^{77,78} the ground state of superfluid helium,⁷⁹ maximally random jammed sphere packings,⁸⁰ and the ground states of spin-polarized fermions.^{81,82}

III. INVERSE METHODS FOR CRYSTAL GROUND STATES

We recall that a classical ground-state configuration \mathbf{r}^N is one that minimizes the system potential energy $\Phi_N(\mathbf{r}^N)$. Our ability to identify ground states for a particular interaction is a highly challenging

problem,^{83,84,85,86,87,88} not to mention the even more difficult inverse problem of designing interactions to achieve targeted ground states. Here we describe recent progress on the latter problem. Because there is a vast (infinitely large) class of many-body potentials, we begin, for simplicity, by considering isotropic pairwise additive interactions, *i.e.*, Eq. (1) reduces to the following form:

$$\Phi_N(\mathbf{r}^N) = \sum_{i < j}^N \varphi(r_{ij}), \quad (3.11)$$

where the *pair potential* $\varphi(r) \equiv \varphi_2(r)$ is a radial function, *i.e.*, it depends on the radial distance $r = |\mathbf{r}|$. Although realistic interactions that operate in soft matter systems can exhibit complicated many-particle characteristics, often a more economical description is sought that uses at most singlet and pair effective interactions that are density dependent to take advantage of the theoretical and computational simplifications that result.⁸⁹ Therefore, our starting point of pairwise additivity (in the absence of an external field) is a practically useful approximation for colloids and polymers, for example.

There are many open questions even for this simple class of potentials. For instance, the limitations of isotropic pairwise additivity for producing target structures are not fully known and can be probed using inverse methods. We know that such interactions cannot produce thermodynamically stable chiral structures with a specified handedness; equal amounts of left-handed and right-handed structures would result. When is anisotropy in the potential required? An answer based on intuition from molecular systems would fail here. For example, the diamond crystal is thought to require directional interactions because such structures found in Nature result from covalent bonding. In fact, it has recently been shown²² that a diamond structure can be created from nondirectional interactions with strong short-range repulsions, as described in detail below. This structure has a special status in photonics research because a diamond crystal of dielectric spheres exhibits a photonic band gap across the Brillouin zone.⁴⁴

Two inverse optimization schemes, called the “zero-temperature” and the “near-melting” schemes,^{18,19} have been devised for the purpose of designing interactions for targeted many-particle configurations. Specifically, the combination of these two optimization techniques lead to an N -body classical system with particles interacting via optimized potentials that has as its ground state (*i.e.*, global energy minimum state) the corresponding target configuration in a specific volume (or density) range. Unlike previous attempts to solve this problem, this conclusion is arrived at only after satisfying four important necessary criteria:

1. lattice sums show that there is a positive pressure (or, equivalently density) range in which the given lattice is stable;

2. all crystal normal mode frequencies are real at a specific density;
3. defects (vacancies and interstitials) are shown to cost the system energy;
4. and the system self-assembles in a molecular dynamics or (Monte Carlo) simulation that starts above the freezing point and is slowly cooled.

As concerns the last criterion, the system may start from an entirely random configuration or with a layer of fixed particles to promote epitaxial growth. Hence we make the important distinction here between homogeneous and heterogeneous nucleation in self-assembly. It is of course a more stringent requirement that the desired lattice self-assemble from a random configuration (homogeneous nucleation). Note that sufficient criteria to ensure that a ground state is exactly achieved do not exist.

A. Zero-Temperature Optimization Scheme

In the zero-temperature optimization scheme, an optimized pair potential for self-assembly of a particular target configuration at a temperature of absolute zero is found by choosing a family of functions $\varphi(r; a_0, a_1, \dots, a_n)$, parametrized by the a_i ’s, and then finding the values of the parameters that lead to the most robust and defect-free self-assembly of the target crystal for a fixed density or, preferably, a range of densities (or, equivalently, a range of pressures). The objective function is chosen so that the energetic stability of a given target crystal is maximized with respect to competitor lattices (chosen previously) subject to the condition that the target crystal is linearly mechanically stable. Mechanical stability is ensured for a given potential by establishing that every phonon mode in the first Brillouin zone is real. Thus, the structure is mechanically stable at zero temperature. However, this does not preclude other structures, periodic or otherwise, from being lower in energy than the targeted one. Therefore, the final outcome of the zero-temperature scheme becomes the initial potential function condition for the near-melting optimization procedure.

B. Near-Melting Optimization Scheme

From an initial parameterized potential (final outcome of the zero-temperature scheme), the near-melting procedure optimizes the potential for self-assembly at a temperature near but below the crystal’s melting point by suppressing nucleation of the liquid phase in molecular dynamics (MD) (or Monte Carlo) simulations. Specifically, simulations are repeatedly run at 80-95% of the melting temperature (the temperature is chosen such

that phase-transition fluctuations do not render the calculations inconsistent), each time calculating the Lindemann parameter, defined by

$$\Theta_2 = \sqrt{\frac{1}{N} \sum_i (\mathbf{r}_i - \mathbf{r}_i^{(0)})^2 - \left(\frac{1}{N} \sum_i (\mathbf{r}_i - \mathbf{r}_i^{(0)}) \right)^2}, \quad (3.12)$$

where \mathbf{r}_i is the position of the i^{th} particle (after an appropriate amount of simulation time), $\mathbf{r}_i^{(0)}$ is its initial position, and N is the number of particles. The parameter Θ_2 is then taken as the objective function for a simulated annealing calculation, and the a_i are found such that Θ_2 is minimized.

The ultimate criterion for self-assembly is the very strong condition that the targeted ground state be observed in a well-annealed molecular dynamics MD simulation starting from the liquid state. The system is slowly annealed to $T = 0$ until the essentially defect-free target crystal results in reasonable computer time. Usually only a very few defects are found at the end of the simulation and its energy is checked to ensure that it is higher than that of the perfect crystal.

IV. OPTIMIZED ISOTROPIC INTERACTIONS FOR LOW-COORDINATED CRYSTAL GROUND STATES

Until recently, conventional wisdom presumed that low-coordinated crystal ground states require directional interactions. The aforementioned optimization schemes were tested initially to yield optimized isotropic (nondirectional) pair potentials that spontaneously yield the four-coordinated square lattice and three-coordinated honeycomb lattice as ground-state structures in two dimensions.^{18,19} The latter target choice is motivated by its three-dimensional analog, the diamond lattice. Figure 1 shows the optimized honeycomb potential and corresponding phonon spectra as well as annealed configuration at $T = 0$. It was found that as long as the salient features of the honeycomb potential are kept (two local minima at distance ratio $\sqrt{3}$, the first being positive and the second negative), self-assembly is unaffected by perturbations in the potential; *i.e.*, the potential is robust. This is an essential feature if this system is to be tested experimentally. We note that the functional form of the optimized “square-lattice” potential is simpler than that of the honeycomb crystal.

In a separate work, the global phase diagram for the optimized “honeycomb” potential was determined.⁹⁰ The phase diagram was obtained from Helmholtz free energies calculated using thermodynamic integration and Monte Carlo simulations. These results showed that the honeycomb crystal remains stable in the global phase diagram even after temperature effects are taken fully into account. Other stable phases in the phase diagram are high- and low-density triangular phases and a fluid phase.

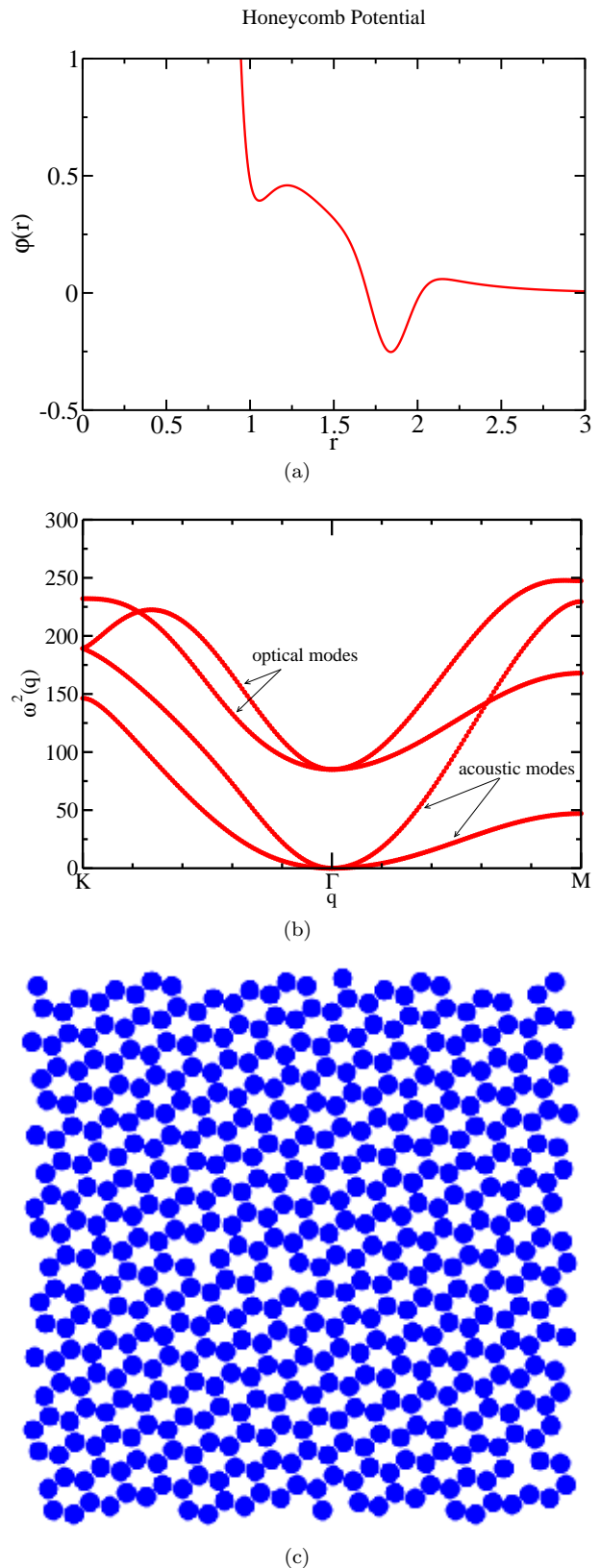


FIG. 1: Honeycomb-crystal self-assembly as obtained in Ref. 18. (a) Optimized pair potential $\varphi(r)$. Dimensionless energy and length units are defined by the axes for this potential. (b) Phonon spectrum (frequency squared) versus wave vector \mathbf{k} for the optimized honeycomb-crystal potential at a specific area equal to 1.45. The acoustic and optical branches are shown. (c) Corresponding 500-particle annealed ground-state configuration. Although there are a few vacancies, these were “frozen in” during annealing due to finite time of the simulation. Such vacancies were shown to cost energy, indicating that the perfect honeycomb crystal is the true ground state.

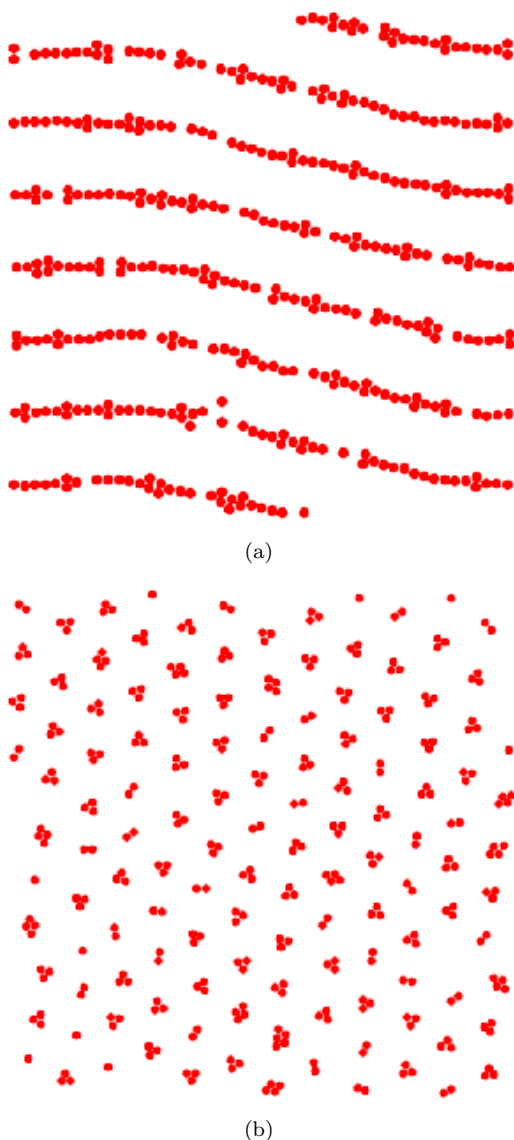


FIG. 2: Unusual two-dimensional ground-state configurations generated from circularly symmetric pair potentials, as adapted from Ref. 19. (a) Chain-like particle configurations. (b) Lattice of “simplex” clusters.

No evidence of gas-liquid or liquid-liquid phase coexistence was found.

In order to test the limitations of circularly symmetric potentials in two dimensions, pair potentials were devised that yielded structurally anisotropic chain-like arrays as well as lattices of compact clusters,¹⁹ as shown in Fig. 2. These structures are reminiscent of “colloidal wires” and “colloidal clusters” found experimentally by the authors of Refs. 5 and 4, respectively. Interestingly, we see that structural anisotropy (colloidal wires) can counterintuitively be achieved with isotropic interactions with the so-called “five-finger” potential.¹⁹ This potential cannot be built in the lab with current technology, but it shows that isotropic potentials have perhaps more flexi-

bility than one would immediately think. It is also very possible that a much simpler isotropic potential could allow for a similar structure to assemble.

These two-dimensional results were extended to the self-assembly of low-coordinated three-dimensional crystals with isotropic pair interactions, including the determination of an optimized pair potential whose classical ground state is the simple cubic lattice and which is functionally simple enough to synthesize in the laboratory.²⁰ The same investigation reported optimized isotropic potentials that yield the body-centered-cubic and simple hexagonal lattices (planes of triangular lattices stacked directly on top of one another), which provide other examples of non-close-packed structures that can be assembled using only isotropic pair interactions.

Optimized isotropic pair-interaction potentials with strongly repulsive cores have been obtained that cause the tetrahedrally coordinated diamond and wurtzite lattices to stabilize, as evidenced by lattice sums, phonon spectra, positive-energy defects, and self-assembly in classical molecular dynamics simulations.²² Figure 3 depicts one self-assembled diamond-crystal configuration shown from three different viewpoints. Finding such a potential via inverse methods is a highly nontrivial problem, since the diamond crystal is extremely close in structure to the tetrahedrally-coordinated *wurtzite* crystal in particular. Given the functional form of the potential, the pressure (or volume) was tuned very precisely to find a small stability range for the diamond structure, and under such conditions, simulations readily demonstrated its self-assembly. These results challenge conventional thinking that such open lattices can only be created via directional covalent interactions observed in nature and adds to our fundamental understanding of the nature of the solid state.

Note that it has been shown that an isotropic pair potential that models star polymer systems has a region of phase stability that favors the diamond crystal.¹⁰ However, this potential, in contrast to the one reported in Ref. 22, possesses a soft core, which would be difficult to synthetically produce using colloids.

V. INVERSE OPTIMIZATION METHODS FOR DISORDERED GROUND STATES

Collective density variables $\rho(\mathbf{k})$ [cf. (2.4)] have proved to be useful tools in the study of static and dynamic phenomena occurring in many-body systems.^{91,92} More recently, the collective-coordinate approach has been used to generate crystalline as well as noncrystalline classical ground states for bounded or “soft” interactions using numerical optimization techniques in two and three dimensions.^{17,27,34} Soft interactions possess great importance in soft-matter systems, such as colloids, microemulsions, and polymers.^{10,11,15,38,43}

We begin by briefly reviewing the basic description of the collective-coordinate approach for N interacting par-

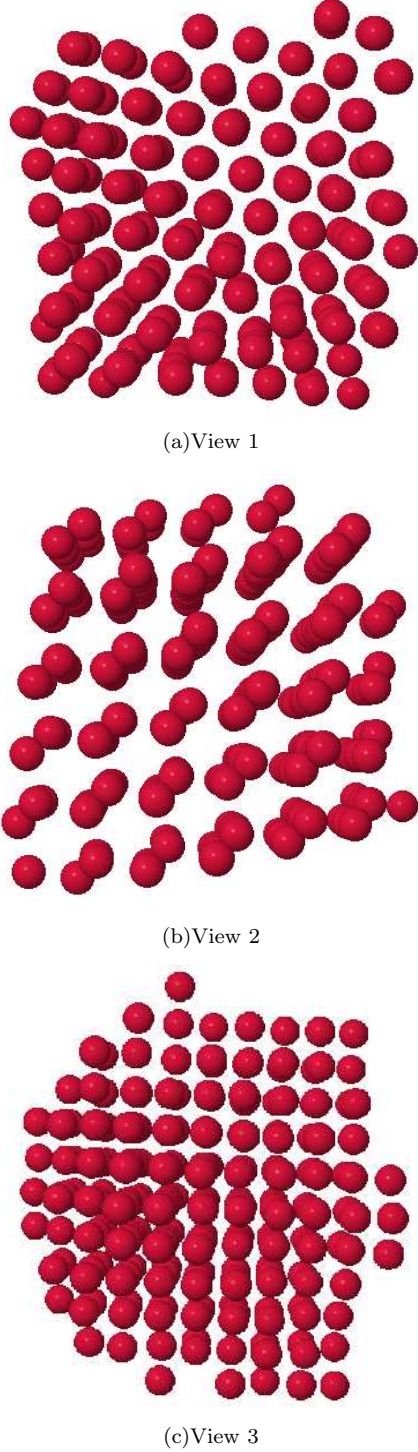


FIG. 3: Results of an MD simulation for 216 particles interacting via the optimized isotropic “diamond” potential showing self-assembly into a perfect diamond configuration, as in Ref. 22. One configuration is shown from three different viewpoints, which clearly show that the result is the diamond crystal.

ticles in a d -dimensional cubic box of side length L and volume Ω under periodic boundary conditions. The corresponding infinite set of wave vectors is given by

$$\mathbf{k} = \left(\frac{2\pi n_1}{L}, \frac{2\pi n_2}{L}, \dots, \frac{2\pi n_d}{L} \right), \quad (5.13)$$

where the n_i ($i = 1, 2, \dots, d$) are positive or negative integers, or zero. The structure factor, defined by (2.5), can be rewritten as follows:

$$S(\mathbf{k}) = \frac{|\rho(\mathbf{k})|^2}{N} = 1 + \frac{2}{N}C(\mathbf{k}),$$

where the real collective density variable $C(\mathbf{k})$ is subject to the following constraints:

$$C(\mathbf{0}) = \frac{1}{2}N(N-1) \quad (5.14)$$

$$C(\mathbf{k}) = C(-\mathbf{k}) \quad (5.15)$$

$$-\frac{1}{2}N \leq C(\mathbf{k}) \leq \frac{1}{2}N(N-1) \quad (\mathbf{k} \neq \mathbf{0}). \quad (5.16)$$

The lower bound on $C(\mathbf{k})$ arises because the structure factor $S(\mathbf{k})$ must be nonnegative.

Let us assume that the total potential energy Φ_N is pairwise additive and therefore given by (3.11). Suppose furthermore that the pair potential $\varphi(r)$ has a Fourier transform $\tilde{\varphi}(\mathbf{k})$:

$$\tilde{\varphi}(\mathbf{k}) = \int_{\Omega} \varphi(\mathbf{r}) \exp(i\mathbf{k} \cdot \mathbf{r}) d\mathbf{r}, \quad (5.17)$$

$$\varphi(\mathbf{r}) = \Omega^{-1} \sum_{\mathbf{k}} \tilde{\varphi}(\mathbf{k}) \exp(-i\mathbf{k} \cdot \mathbf{r}), \quad (5.18)$$

where in the last expression the summation covers the entire set of \mathbf{k} 's. Then it is straightforward to show that the total potential energy for the N -particle system can be exactly expressed in the following manner in terms of the real collective density variables

$$\Phi_N(\mathbf{r}^N) = \Omega^{-1} \sum_{\mathbf{k}} \tilde{\varphi}(\mathbf{k}) C(\mathbf{k}). \quad (5.19)$$

Consider pair interactions whose transform $\tilde{\varphi}(\mathbf{k})$ is non-negative radial function $f(k) \geq 0$ ($k = |\mathbf{k}|$) with compact support, *i.e.*,

$$\tilde{\varphi}(k) = f(k)\Theta(K - k), \quad (5.20)$$

where

$$\Theta(x) = \begin{cases} 0, & x < 0, \\ 1, & x \geq 0, \end{cases} \quad (5.21)$$

is the Heaviside step function. We see that if the $C(\mathbf{k})$ is driven to its minimum value $-N/2$ for $|\mathbf{k}| < K$, then that configuration must be a classical ground state of the system, the absolute minimum of Φ . Thus, density fluctuations for those \mathbf{k} 's such that $|\mathbf{k}| < K$ are completely suppressed, *i.e.*, the structure factor $S(\mathbf{k}) = 0$ for

$|\mathbf{k}| < K$. Note that for the form (5.20), the corresponding real-space pair potential $\varphi(r)$ will be an oscillating potential. However, there are choices for $f(k)$ one can make, especially for purposes of experimental realizability, that can appreciably dampen the amplitudes and range of the real-space interactions.

Although the number of collective variables is infinite, the N -particle system possesses only dN configurational degrees of freedom, where d is the Euclidean space dimension. Consequently, it is unreasonable to suppose (barring special circumstances) that generally all $C(\mathbf{k})$'s could be independently controlled. However, it is possible, as illustrated below, to specify simultaneously a number of the collective variables equal to a significant fraction of dN . We denote by χ the ratio of the constrained degrees of freedom to the total number of degrees of freedom. As χ increases to cover larger and larger numbers of the wave vectors, and consequently having an impact on a larger and larger fraction of the total degrees of freedom, the result for the classical ground state is far from obvious. It is clear that if χ is a fraction of order unity, the ground state is periodic, which has been established.^{17,27,34,86,92}

However, the more interesting cases involve disordered ground states (*i.e.*, configurations that possess no long-range order), which arise for a range of $\chi \in [0, \chi_{max}]$, provided that χ_{max} is sufficiently small.^{17,27,34} Our primary interest here are in the disordered, degenerate ground states that can be produced by the collective-density approach. Such systems have the remarkable property of being able to self-assemble into one of the numerous degenerate disordered configurations when slowly cooled to absolute zero.

For any given choice of N and K , the numerical procedure utilizes a random number generator to create an initial configuration of the particles inside the hypercubic box. This starting point typically produces a large positive value of the system potential energy Φ_N . The next step involves use of an optimization procedure, such as the conjugate gradient method or a more sophisticated technique,³⁴ to seek a particle configuration that yields the absolute minimum value of Φ_N .

This numerical optimization technique has been employed to generate two-dimensional classical ground-state particle configurations with the simple transform choice $f(k) = 1$ in (5.20), *i.e.*, the pure unit step function, which is zero for $k > K$.¹⁷ The resulting investigation distinguished three structural regimes as the number of constrained wave vectors is increased (*i.e.*, as χ is increased) - disordered, wavy crystalline, and crystalline regimes.

The aforementioned collective-coordinate procedure has been generalized to those cases in which $C(\mathbf{k})$ is constrained to be some target value $C_0(\mathbf{k}) \geq 0$ for $\mathbf{k} \in \mathbf{Q}$, where \mathbf{Q} represents the finite set of \mathbf{k} 's for which a number of the collective density variables can simultaneously be specified. Of course, each $C_0(\mathbf{k})$ must lie in the range specified by inequalities of (5.16). Then consider the fol-

lowing non-negative objective function:

$$\Phi_N(\mathbf{r}^N) = \sum_{\mathbf{k} \in \mathbf{Q}} \tilde{\varphi}(\mathbf{k}) [C(\mathbf{k}) - C_0(\mathbf{k})]^2. \quad (5.22)$$

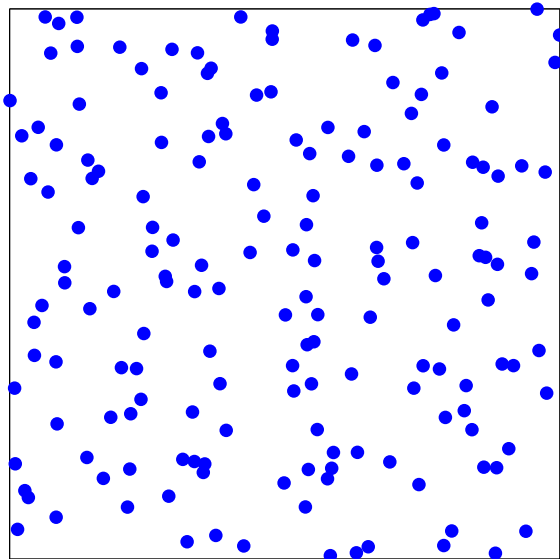
If Φ_N is interpreted as a potential energy of interaction for the N point particles, then it can be shown that it represents intrinsic two-body, three-body and four-body interaction potentials operating in the system. If classical ground-state configurations for the N particles subject to that potential exist for which $\Phi_N = 0$, then those configurations necessarily attain the desired target values of the collective variables.

This generalization of the collective coordinate approach was applied in three dimensions.²¹ In particular, multi-particle configurations were generated for which $S(\mathbf{k}) \propto |\mathbf{k}|^\alpha$, $|\mathbf{k}| \leq K$, and $\alpha = 1, 2, 4, 6, 8$, and 10. The case $\alpha = 1$ is relevant for the Harrison-Zeldovich model of primordial density fluctuations of the early Universe,^{77,78} superfluid helium,⁷⁹ maximally random jammed sphere packings,⁹³ and spin-polarized fermions.^{81,82} This analysis also provides specific examples of interaction potentials whose classical ground states for finite-sized systems are configurationally degenerate and disordered.

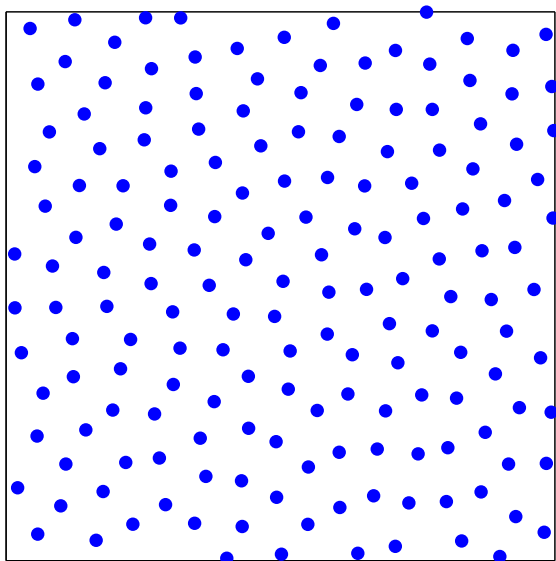
Employing this collective-coordinate numerical optimization procedure, ground-state configurations of interacting particle systems in the first three space dimensions have been constructed so that the scattering of radiation exactly matches a prescribed pattern for a set of wave vectors.²⁷ It is demonstrated that the constructed ground states are, counterintuitively, disordered (*i.e.*, possess no long-range order) in the *infinite-volume* limit. Three classes of configurations with unique radiation scattering characteristics were studied: (i) "stealth" materials, which are transparent to incident radiation at certain wavelengths; (ii) "super-ideal" gases, which scatter radiation identically to that of an ensemble of ideal gas configurations for a selected set of wave vectors; and (iii) "equi-luminous" materials, which scatter radiation equally intensely for a selected set of wave vectors.

Although stealth materials and super-ideal gases are subsets of equi-luminous materials, we use this term to refer to materials that scatter radiation more intensely relative to an ideal gas. These materials that scatter radiation much more intensely than an ideal gas for a set of wave vectors have enhanced density fluctuations and show local clustering similar to polymers and aggregating colloids.^{94,95} With the collective-coordinate inverse procedure, the degree of clustering can be imposed by tuning the scattering characteristics for certain wavelengths.

For purposes of illustration, disordered "stealth" configurations are depicted in two dimensions in Figure 4 for 168 particles for two selected values of χ . At the lowest χ considered, the configuration is seen not to have strong spatial correlations. At highest χ value reported, the particles develop an exclusion shell about their centers but the system still does not possess any long-range order. A system size study was carried out that revealed



(a)



(b)

FIG. 4: Stealth particle patterns of 168 particles in two dimensions, as adapted from Ref. 27: (a) $\chi = 0.04167$, (b) $\chi = 0.20238$. Both systems are disordered but at higher χ , particles tend to repel one another to a greater degree. The potential energy was minimized to within 10^{-17} of its global minimum.

no long-range order when extrapolated to the infinite-volume limit.

VI. DUALITY RELATIONS FOR CLASSICAL GROUND STATES

The determination of the classical ground states of interacting many-particle systems (global minimum energy configurations) is an outstanding problem in condensed-matter physics and materials science.^{83,84} While classical ground states are readily produced by slowly freezing liquids in experiments and computer simulations, our theoretical understanding of them is far from complete.

Much of the progress to rigorously identify ground states for given interactions has been done for lattice models, primarily in one dimension.⁸⁴ The solutions in d -dimensional Euclidean space \mathbb{R}^d for $d \geq 2$ are considerably more challenging. For example, the ground state(s) for the well-known Lennard-Jones potential in \mathbb{R}^2 or \mathbb{R}^3 are not known rigorously (although many computer simulations support the conclusion that the hexagonal close-packed crystal is its ground state).

Soft (bounded) interactions are easier to treat theoretically as evidenced by recent progress in our understanding of ground states of this class of potentials in \mathbb{R}^2 and \mathbb{R}^3 .^{17,27,34,86,87} Moreover, as we noted earlier, such interactions possess great importance in a variety of soft-matter systems.^{10,11,15,38,43}

Nonetheless, new theoretical tools are required to make further progress. Duality relations that link the energy of configurations associated with a class of soft pair potentials to the corresponding energy of the dual (Fourier-transformed) potential have recently been derived.⁸⁸ These duality relations enable one to use information about ground states of short-ranged potentials to draw new conclusions about the nature of the ground states of long-ranged potentials and vice versa. Among other results, they also have led to the identification of unusual one-dimensional systems with ground-state “phase transitions” and can be employed to make computational searches for ground states more efficient.

Before discussing these duality relations, which take the form of two theorems, we introduce some notation. Let $U(\mathbf{r}^N)$ be twice the total potential energy per particle in an N -particle system with pairwise interactions, *i.e.*,

$$U(\mathbf{r}^N) = \frac{1}{N} \sum_{i,j} \varphi(r_{ij}), \quad (6.23)$$

where $\varphi(r)$ is a radial pair potential function and $r_{ij} = |\mathbf{r}_j - \mathbf{r}_i|$. A *classical ground-state* configuration is one that minimizes $U(\mathbf{r}^N)$. We consider those stable radial pair potentials $\varphi(r)$ that are bounded and absolutely integrable and call such functions admissible. Thus, the corresponding Fourier transform $\tilde{\varphi}(k)$ in d dimensions at wave number k exists. We recall that in a Bravais lattice Λ , the space \mathbb{R}^d can be geometrically divided into identical regions called *fundamental cells*, each of which contains one particle center.⁹⁶ We denote the reciprocal Bravais lattice by $\tilde{\Lambda}$. If the Bravais lattice Λ has density ρ , then its reciprocal lattice $\tilde{\Lambda}$ has density $\tilde{\rho} = \rho^{-1}(2\pi)^{-d}$.

Theorem 1. *If an admissible pair potential $\varphi(r)$ has a Bravais lattice Λ ground-state structure at number density ρ , then we have the following duality relation for twice the minimized energy per particle U_{min} :*

$$\varphi(r=0) + \sum'_{\mathbf{r} \in \Lambda} \varphi(r) = \rho \tilde{\varphi}(k=0) + \rho \sum'_{\mathbf{k} \in \tilde{\Lambda}} \tilde{\varphi}(k), \quad (6.24)$$

where the prime on the sum denotes the zero vector should be omitted, $\tilde{\Lambda}$ denotes the reciprocal Bravais lattice, and $\tilde{\varphi}(k)$ is the dual pair potential, which automatically satisfies the stability condition, and therefore is admissible. Moreover, twice the minimized energy per particle \tilde{U}_{min} for any ground-state structure of the dual potential $\tilde{\varphi}(k)$, is bounded from above by the corresponding real-space minimized quantity U_{min} or, equivalently, the right side of (6.24), i.e.,

$$\tilde{U}_{min} \leq U_{min} = \rho \tilde{\varphi}(k=0) + \rho \sum'_{\mathbf{k} \in \tilde{\Lambda}} \tilde{\varphi}(k). \quad (6.25)$$

Whenever the reciprocal lattice $\tilde{\Lambda}$ at reciprocal lattice density $\tilde{\rho} = \rho^{-1}(2\pi)^{-d}$ is a ground state of $\tilde{\varphi}(k)$, the inequality in (6.25) becomes an equality. On the other hand, if an admissible dual potential $\tilde{\varphi}(k)$ has a Bravais lattice $\tilde{\Lambda}$ at number density $\tilde{\rho}$, then

$$U_{min} \leq \tilde{U}_{min} = \tilde{\rho} \varphi(r=0) + \tilde{\rho} \sum'_{\mathbf{r} \in \Lambda} \varphi(r), \quad (6.26)$$

where equality is achieved when the real-space ground state is the lattice Λ reciprocal to $\tilde{\Lambda}$.

Whenever equality in relation (6.25) is achieved, then a ground state structure of the dual potential $\tilde{\varphi}(k=r)$ evaluated at the real-space variable r is the Bravais lattice $\tilde{\Lambda}$ at density $\tilde{\rho} = \rho^{-1}(2\pi)^{-d}$. Theorem 1 leads to another theorem (both of which are proved in Ref. 88) concerning phase coexistence.

Theorem 2. *Suppose that for admissible potentials there exists a range of densities over which the ground states are side by side coexistence of two distinct crystal structures whose parentage are two different Bravais lattices, then the strict inequalities in (6.25) and (6.26) apply at any density in this density-coexistence interval.*

Note that the ground states referred to in Theorem 2 are not only non-Bravais lattices, they are not even periodic. The ground states are side-by-side coexistence of two crystal domains whose shapes and relative orientations are complicated functions of ρ .

On account of the “uncertainty principle” for Fourier pairs, a non-localized (long-ranged) potential $\varphi(r)$ has a corresponding localized (compact) dual potential $\tilde{\varphi}(k)$. Similarly, a localized (compact) potential $\varphi(r)$ has a corresponding non-localized (long-ranged) dual potential $\tilde{\varphi}(k)$. This property of Fourier pairs and the duality relations of Theorem 1 enable one to use information about

ground states of short-ranged potentials to draw new conclusions about the nature of the ground states of long-ranged potentials and vice versa. In particular, three different classes of admissible potential functions have been considered: (1) *compactly* supported functions (such as the ones employed in the collective-coordinate approach discussed in Section V); (2) *nonnegative* functions; and (3) *completely monotonic* functions.

For purposes of illustration, we discuss here in some detail, the application of Theorem 1 to the class potential functions that have been used in the collective-coordinate approach reviewed in Section V. Recently, the ground states corresponding to a certain class of oscillating real-space potentials $\varphi(r)$ as defined by the family of Fourier transforms with compact support such that $\tilde{\varphi}(k)$ is positive for $0 \leq k < K$ and zero otherwise have been studied.^{17,86} Clearly, $\tilde{\varphi}(k)$ is an admissible pair potential. In Ref. 86, it was shown that in three dimensions the corresponding real-space potential $\varphi(r)$, which oscillates about zero, has the body-centered cubic (bcc) lattice as its unique ground state at the real-space density $\rho = 1/(8\sqrt{2}\pi^3)$ (where we have taken $K = 1$). Moreover, it was demonstrated⁸⁶ that for densities greater than $1/(8\sqrt{2}\pi^3)$, the ground states are degenerate such that the face-centered cubic (fcc), simple hexagonal (sh), and simple cubic (sc) lattices are ground states at and above the respective densities $1/(6\sqrt{3}\pi^3)$, $\sqrt{3}/(16\sqrt{2}\pi^3)$, and $1/(8\sqrt{2}\pi^3)$.

Because all of the aforementioned ground states are Bravais lattices, the duality relation (6.24) can be applied to infer the ground states of real-space potentials with compact support. Specifically, application of the duality theorem in \mathbb{R}^3 and the results of Ref. 86 enables us to conclude that for the real-space potential $\varphi(r)$ that is positive for $0 \leq r < D$ and zero otherwise, the fcc lattice (dual of the bcc lattice) is the unique ground state at the density $\sqrt{2}$ and the ground states are degenerate such that the bcc, sh and sc lattices are ground states at and below the respective densities $(3\sqrt{3})/4$, $2/\sqrt{3}$, and 1 (taking $D = 1$). Specific examples of such real-space potentials, for which the ground states are not rigorously known, include the “square-mound” potential [$\varphi(r) = \epsilon > 0$ for $0 \leq r < 1$ and zero otherwise] and the “overlap” potential $\alpha(r; D/2)$,⁷² equal to the intersection volume of two d -dimensional spheres of diameter D whose centers are separated by a distance r divided by the volume of a sphere (discussed in Section II), and thus has support in the interval $[0, D)$. Moreover, any structure, periodic or not, in which the nearest-neighbor distance is greater than unity is a ground state.

Importantly, at densities corresponding to nearest-neighbor distances that are less than unity, the possible ground-state structures is considerably more difficult to ascertain. For example, it has been argued in Ref. 43 (with good reason) that real-space potentials whose Fourier transforms oscillate about zero will exhibit polymorphic crystal phases in which the particles that comprise a cluster sit on top of each other. The square-mound

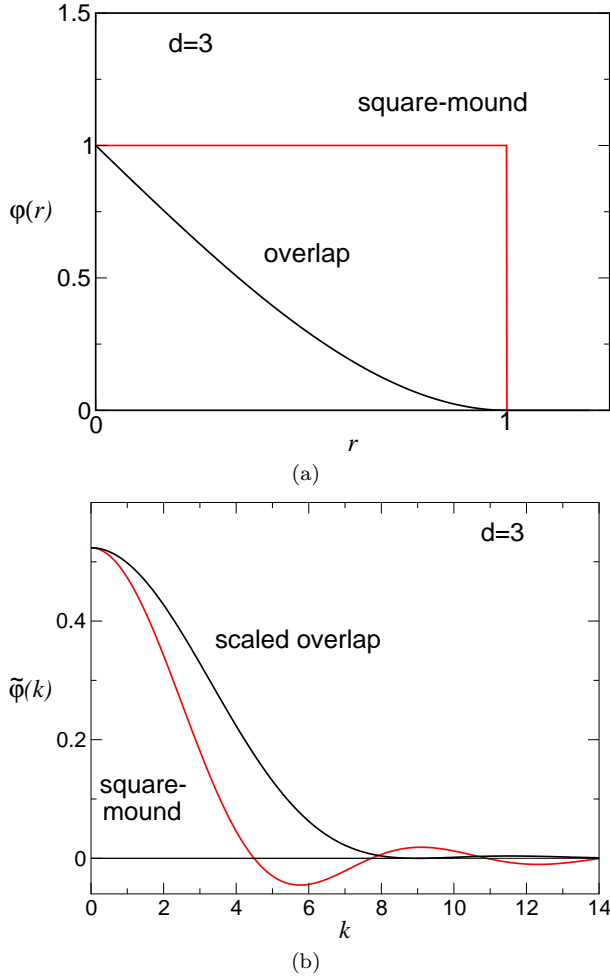


FIG. 5: (a) The localized square-mound potential [$\varphi(r) = \epsilon = 1$ for $0 \leq r < 1$ and zero otherwise] and overlap potential [$\varphi(r) = 1 - 3r/2 + r^3/2$ for $0 \leq r < 1$ and zero otherwise] in \mathbb{R}^3 . (b) The delocalized dual square-mound potential $\tilde{\varphi}(k) = \pi^{3/2} J_{3/2}(k)/(2k)^{3/2}$ multiplied by $\pi^3/6$ and dual overlap potential $\tilde{\varphi}(k) = 6\pi^2 J_{3/2}^2(k/2)/k^3$.

potential is a special case of this class of potentials and the fact that it is a simple piecewise constant function allows for a rigorous analysis of the clustered ground states for densities in which the nearest-neighbor distances are less than the distance at which the discontinuity in $\varphi(r)$ occurs.

The duality relations have also led to the identification of a one-dimensional system that exhibits an infinite number of “phase transitions” at $T = 0$ from Bravais to non-Bravais lattices over the entire density range as well as a conjecture regarding the ground states of purely repulsive monotonic potentials.⁸⁸ Moreover, inequalities (6.25) and (6.26) provide a computational tool to estimate ground-state energies or eliminate candidate ground-state structures as obtained from annealing simulations.

The Gaussian potential is a special case of a purely re-

pulsive monotonic potential, and is a useful interaction to model polymer systems.^{11,43} The phase diagram of such systems in various spatial dimensions has recently been investigated⁹⁷ in order to understand the effect of dimensionality, apply the aforementioned duality relations, and to test a conjecture of Ref. 88 concerning completely monotonic potentials. The Gaussian potential is an example of the class of potentials in which both the real-space and dual potentials are nonnegative functions. The authors of Ref.⁴³ have argued that such systems display re-entrant melting with an upper freezing temperature.

Elsewhere, corresponding duality relations for potential functions that also include three-body and higher-order interactions will be derived⁹⁸.

VII. CONSTRUCTION OF CONFIGURATIONS WITH TARGET PAIR CORRELATIONS

The subject of atomic and molecular distribution functions has enjoyed a long and rich history. However, not surprisingly for a scientific area so characterized by intrinsic complexity, some deep problems of incomplete understanding still persist.

One such open question concerns realizability of a given candidate pair correlation function $g_2(\mathbf{r})$, namely, whether it actually represents the pair correlation of some many-particle configuration at number density $\rho > 0$. This is called the *realizability* problem.^{30,72} Several necessary conditions that must be satisfied by the candidate are known, including nonnegativity of $g_2(\mathbf{r})$ and its associated structure factor $S(\mathbf{k})$, as well as constraints on implied local density fluctuations.⁹⁹ It has recently come to light that a positive g_2 at a positive ρ must satisfy an uncountable number of necessary and sufficient conditions for it to correspond to a realizable point process.^{100,101} However, these conditions are very difficult (or, more likely, impossible) to check for arbitrary dimension. In other words, given ρ and g_2 , it is difficult to ascertain if there are some higher-order functions g_3, g_4, \dots for which these one- and two-particle correlation functions hold.

To shed light on the realizability problem, a simple one-dimensional lattice model, with single-site occupancy, and nearest-neighbor exclusion has been investigated.³² The following results were obtained: (a) pair correlation realizability over a nonzero density range, (b) violation of the Kirkwood superposition approximation for g_3 , and (c) inappropriateness of the so-called “reverse Monte Carlo” method that uses a candidate pair correlation function as a means to suggest typical many-body configurations. Note that Chayes and Chayes¹⁰² proved that for any pair correlation function (meeting mild conditions) that is derivable from an N -body Hamiltonian, there always exists a unique “effective” two-body potential that produces the same pair correlation function (but generally not the higher-body correlation function g_3, g_4, g_5 , etc.). This theorem has been successfully applied to polymer solutions to obtain effective pair inter-

actions from g_2 ^{103,104}.

Elsewhere, so-called iso- g_2 processes were studied in the equilibrium regime. These consist of a sequence of equilibrium many-body systems that have different number densities but share, at a given temperature, the same “target” pair correlation function. In other words, in these processes, density-dependent interactions identically cancel the usual density variation of many-body pair correlation functions.^{28,29,33} Target pair correlation functions studied include the unit step function as well as the zero-density limit of the square-well potential (for which $g_2(r) = \exp[-\beta\varphi(r)]$). Formal density expansions for effective pair potentials were derived with this iso- g_2 property, showing how successive terms in that expansion can be determined iteratively. Explicit results through second density order have been obtained for two types of “target” pair correlation functions, and the conditions under which realizability can be attained were explored.³³

In order to explore and gain insight into the basic statistical geometric features of random sphere packings, the notion of a g_2 -invariant process was introduced.³⁰ A g_2 -invariant process is one in which a given nonnegative pair correlation $g_2(\mathbf{r})$ function remains invariant as density varies for all \mathbf{r} over the range of densities

$$0 \leq \rho \leq \rho_*. \quad (7.27)$$

The terminal density ρ_* is the maximum achievable density for the g_2 -invariant process subject to satisfaction of the known necessary conditions on the pair correlation function. The determination of the terminal density for various forms of g_2 that putatively correspond to a sphere packing has been solved using numerical and analytical optimization techniques.^{30,35,36,37}

To test whether such g_2 's at terminal density ρ_* are indeed realizable by sphere packings, stochastic optimization techniques originally, developed to construct material microstructures with targeted lower-order correlation functions,^{105,106,107} were employed.^{31,34} In a construction algorithm, an initial configuration of particles evolves such that the final configuration possesses a set of targeted correlation functions up to some “cut-off” distances. This is done by choosing the objective function to be a “squared error” involving the set of targeted correlation functions. The evolving configurations are induced by minimizing this objective function via a stochastic optimization procedure.

For example, for the case of d -dimensional packing of congruent spheres of diameter D in which the pair correlation function is taken to be

$$g_2(r) = \frac{Z}{\rho s_1(r)} \delta(r - D) + \Theta(r - D), \quad (7.28)$$

where Z represents the average contact value per sphere and $s_1(r) = d\pi^{d/2}r^{d-1}/\Gamma(1 + d/2)$ is the surface area of a d -dimensional sphere,³⁰ it was found that the terminal packing fraction ϕ_* (fraction of space covered by the

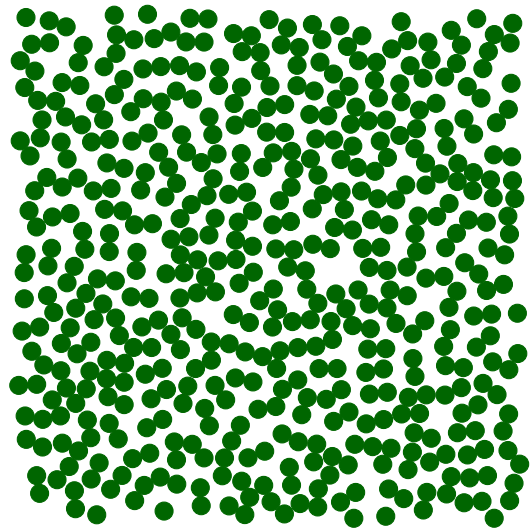
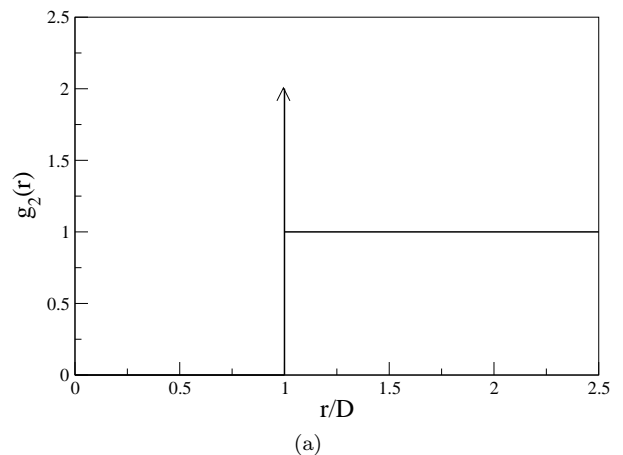


FIG. 6: (a) Graph of the target pair correlation function $g_2(r)$: Dirac δ function plus a step function. (b) A two-dimensional configuration of 500 particles that realizes this targeted form for $g_2(r)$ up to a dimensionless distance of $r/D = 2.5$, as adapted from Ref. 34. The configuration consists of only dimers at the terminal packing fraction $\phi_* = 0.5$ with an average contact value $Z = 1.0$.

spheres) and the associated average contact number Z_* are given by

$$\phi_* = \frac{d+2}{2^{d+1}}, \quad Z_* = \frac{d}{2}. \quad (7.29)$$

Numerical evidence suggests that such a pair correlation is achieved by a single sphere packing configuration for any $d \geq 2$.³⁴ Such a pair correlation function Figure 6 shows a realization of such a packing in two dimensions. Of course, in any simulation, pair distances must binned and sampled up to some cut-off distance. Note that for a sufficiently large system, the targeted correlation for a single configuration approaches that of one obtained

from an ensemble of configurations by ergodicity.

Because the realizability problem is far from being solved, it remains an active area of research. For example, it has been conjectured that any radial, nonnegative pair correlation function characterized by a hard-core, which decays sufficiently rapidly to unity, is realizable by a translationally invariant disordered sphere packing in d -dimensional Euclidean space for asymptotically large d if and only if $S(k) \geq 0$.¹⁰⁸ Although there is mounting evidence to support this conjecture,^{35,37,108} a proof of it is a great challenge.

VIII. DESIGNING ISOTROPIC PAIR POTENTIALS FOR TARGETED BULK PROPERTIES

Inverse methods have been recently devised to optimize interactions of many-particle systems to achieve targeted novel bulk properties. To illustrate the interesting possibilities, we discuss three specific target examples in some detail: the thermal expansion coefficients and Poisson's ratio.

A. Thermal Expansion Coefficients

Control of thermal expansion properties of materials is of technological importance due the need for structures to withstand ambient temperature variations. In the technological realm, materials with zero thermal expansion (those that do not expand or contract upon heating) can aid in the longevity of space structures, bridges and piping systems.^{50,109} Materials with very large thermal expansion coefficients could function as actuators, and those with negative thermal expansion coefficients may be of use as thermal fasteners.⁴⁸

Negative thermal expansion (NTE) behavior, a well-known but unusual phenomenon in many-particle systems, has been observed only in multi-component materials with open unit cell structures in which the bonding of component particles is highly directional. Perhaps the most common example of a solid exhibiting NTE is that of ice, which contracts upon melting into liquid water.¹¹⁰ Another example of a material that undergoes NTE is zirconium tungstate, ZrW_2O_8 , which exhibits this behavior for an extremely large temperature range, namely 0.3K through 1050K.¹¹¹

An isotropic interaction potential has been optimized that gives rise to negative thermal expansion (NTE) behavior in equilibrium many-particle systems in the solid state in both two and three dimensions over a wide temperature and pressure range (including zero pressure).²³ Although such anomalous behavior is well-known in materials with directional interactions (*e.g.*, zirconium tungstate), this is the first time that NTE behavior has been established to occur in the solid state of single-component many-particle systems for isotropic in-

teractions. (Note that NTE has been shown to occur in a two-dimensional *fluid* with isotropic interactions.^{112,113}) Moreover, it was established that a sufficient condition for a potential to give rise to a system with NTE behavior is that it exhibits a softened interior core within a basin of attraction (as depicted schematically in part (a) of Fig. 7). Using an optimization procedure to find a potential that yields a strong NTE effect and constant-pressure Monte Carlo simulations, it was shown that as the temperature was increased, the “softened interior core” potential [part (b) of Fig. 7], the system exhibited negative, zero, and then positive thermal expansion before melting (in both two and three dimensions).

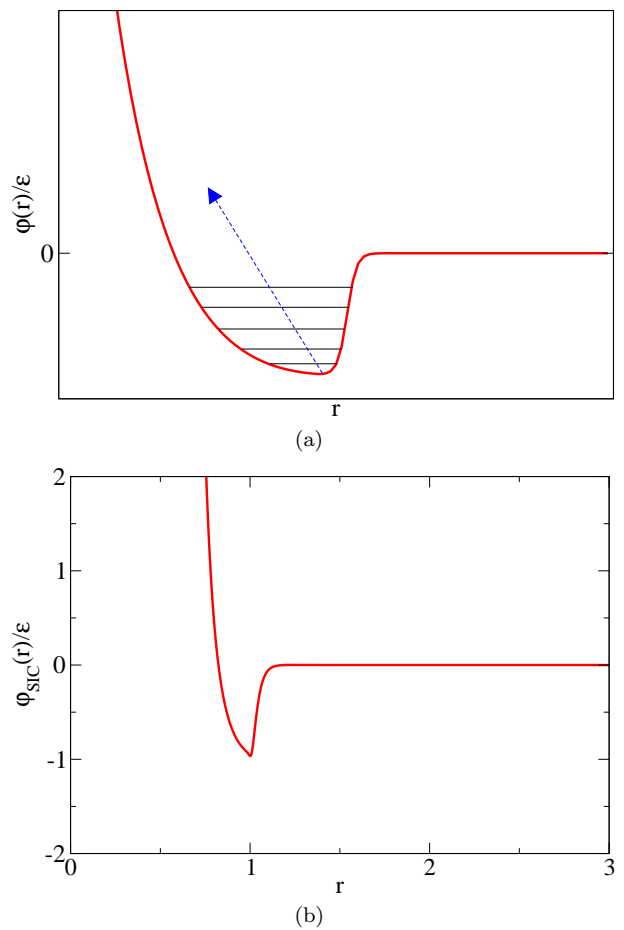


FIG. 7: (a) Schematic depiction of an isotropic pair potential (scaled by the well depth ϵ) with a softened interior in its basin of attraction following Ref. 23. Thermal fluctuations cause the average nearest-neighbor distance to decrease, resulting in an overall contraction of the system upon heating. (b) The optimized “softened interior core” (SIC) potential, as adapted from Ref. 23, has NTE behavior over a wide range of temperatures.

B. Poisson's Ratio

Another interesting target bulk property is the Poisson's ratio ν . In particular, it is desired to optimize interactions to achieve negative Poisson's ratio (NPR), the so-called "auxetic" materials^{114,115}. When such materials are stretched in a particular direction, they expand in an orthogonal direction. Auxetic behavior is a counter intuitive material property that has been observed only in a handful of elastically isotropic materials that often have intricate structures and characteristic lengths much larger than an atomic bond length, such as foams⁵¹ and other cellular materials.^{52,53,54,56} Auxetic materials have a great deal of technological potential; for example, they can be used as strain amplifiers.¹¹⁵ If auxetic materials are used as a matrix in the manufacture of miniature sensors based on piezoceramic composites, the range of operating frequencies of a piezoelectric transducer is widened and the sensitivity of the device is increased.¹¹⁶ They can also be used as mechanical components of microelectromechanical systems, and as transducing structures, shock absorbers and fasteners.⁵⁶

It has been recently found that under *tension* (*i.e.*, negative pressure), many-body two- and three-dimensional systems with isotropic two-body interaction potentials can have a negative Poisson's ratio in the crystal phase as long as certain linear equalities and inequalities involving the interaction potential $\varphi(r)$ are satisfied.²⁶ This is an unexpected result, since it describes an inherently anisotropic behavior that arises from isotropic interactions; indeed, most previously discovered auxetic materials exhibit complex, carefully designed anisotropic interactions. This can be shown to be the case at zero temperature for the elastically isotropic triangular lattice in two dimensions, and for the fcc lattice in three dimensions, which, surprisingly, can also be made to be elastically isotropic. One can show that in the former case, the simple Lennard-Jones potential can give rise to auxetic behavior (see Fig. 8). In the three-dimensional case, auxetic behavior is exhibited even when the elastic constants are constrained such that the material is elastically isotropic. Finding auxetic behavior over a wide range in temperature and pressure is a challenging *optimization* problem that has yet to be addressed.

This analysis suggests that auxetic behavior only occurs in crystals under the nonequilibrium condition of negative pressures when the system contains only pair interactions and is elastically isotropic. Such auxetic materials may potentially be experimentally produced using synthetic techniques that rely on kinetic effects; examples include tempered glass,¹¹⁷ and even colloidal crystals.¹¹⁸ However, a three-body potential has been devised that yields NPR behavior in close-packed two- and three-dimensional lattices by construction at zero temperature and positive pressure.²⁶ In order to produce this behavior, the potential has a built-in energy cost associated with deforming the equilateral triangles in the two-dimensional triangular lattice and the three-dimensional

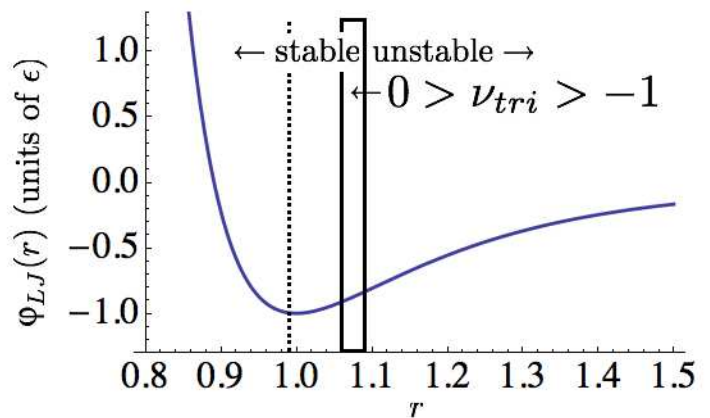


FIG. 8: Region of lattice constants (indicated by the rectangular box) for which the Poisson's ratio is negative in a triangular lattice, using the Lennard-Jones interaction potential, φ_{LJ} , as adapted from Ref. 26. Pressure is positive to the left of the dotted line and negative to the right; thus, auxetic behavior only occurs at *negative pressure*. To the right of the rectangular box, the lattice becomes unstable.

close-packed lattices. The interested reader is referred to Ref. 25 for the explicit form of this three-body potential.

IX. FUTURE WORK AND CONCLUSIONS

In this section, we discuss future directions and close with concluding remarks.

A. Interaction Potentials for Targeted Configurations at Positive Temperature

Most of the inverse techniques reviewed here were directed toward obtaining ground state ($T = 0$) structures. However, the same methods can be extended to treat many-particle configurations at positive temperature. For example, an ability to control the formation of point, line, and planar defects of crystals under various growth conditions at positive temperature is highly desirable. The required interactions to achieve representative amorphous target structures, including equilibrium liquids at positive temperature and low-temperature glasses, is another interesting application.

B. Interaction Potentials for Targeted Multicomponent Systems

It is straightforward to extend the zero-temperature and near-melting optimization schemes^{18,19} to multicomponent systems. The parameter space, which now includes species composition and effective particle size ra-

tios, becomes much larger than the single-component instance, and therefore one must be careful in selecting the family of potential functions that must be optimized as well as the target structures. In order to make the search manageable, one could limit the choice of potential functions to those that are consistent with interparticle interactions found in colloidal systems. In addition to hard-sphere-like interactions, these include long-range repulsive, short-range attractive and averaged dipolar interactions. It has recently been shown that the electrostatic interaction between oppositely charged particles, which are long-range attractive interactions, can result in a rich class of stable ionic colloidal crystals,¹⁴ as illustrated Figure 9. Motivated by this remarkable investigation, one can imagine optimizing a family of potential functions based on such interactions that target an even broader class of crystal structures.

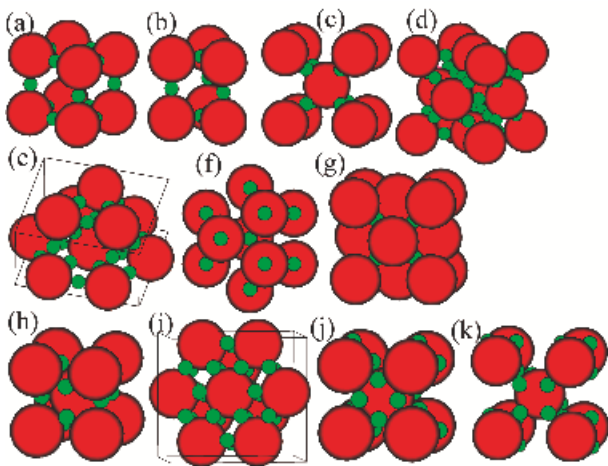


FIG. 9: Theoretically predicted stable binary crystals of oppositely charged colloids with different stoichiometries, as obtained from Ref. 14 (with the permission of the authors).

C. Anisotropic Interactions

We have seen that there exists nontrivial families of radial pair potentials for which interesting targeted structures are the stable low-temperature forms. Consequently, it was not necessary in principle to call upon angle-dependent or non-additive interactions to form such nonconventional lattices. However, anisotropic pair interactions offer greater flexibility to achieve targeted structures and therefore provides a new direction to apply our inverse methods.

Recently, a new generation of colloidal particles with chemically or physically patterned surfaces has been designed and synthesized in the attempt to manipulate the valency of the colloidal particles.^{4,119,120} This synthesis effort aims to generate “superatoms” (*i.e.*, atoms at the nano and microscopic length scales) in order to reproduce and extend traditional collective molecular behav-

ior to larger length scales; thus, opening the new eld of “supra-particle” colloidal physics.

One simple way to model such interactions is via “patchy” particles, *i.e.*, particles with discrete, attractive interaction sites at prescribed locations on the particle surface. Molecular simulations have been carried out to investigate the self-assembly of patchy particles.^{12,16,121} Chains, sheets, rings, icosahedra, square pyramids, tetrahedra, and twisted and staircase structures have been obtained through suitable design of the surface pattern of patches. Patchy particles represent a new class of building blocks for the fabrication of colloids with unique structural characteristics.

Thus, it would be highly desirable to optimize patchy particles interactions to achieve low-coordinated crystal structures, amorphous structures, and quasicrystals. Again, this can be accomplished by appropriate simple extensions of the zero-temperature and near-melting optimization schemes that were originally implemented for isotropic interactions.

D. Inverse Optimization Methods for Novel Targeted Bulk Properties

A full-blown and general optimization scheme that can be used to find optimized interactions over a large family of potential functions for a given set of bulk properties over a wide range of conditions has yet to be devised. For example, optimizing interactions in a many-particle system so that it exhibits auxetic behavior over a wide range in temperature and pressure is a challenging problem. One path toward the general goal is to formulate a methodology that incorporates a set of bulk properties in the objective function in the same spirit as has been done for topology optimization of composite materials,^{48,59,61,109} but in a molecular dynamics simulation. Specifically, the objective function can either be the bulk property itself (which is extremized) or a squared “error” function involving a targeted bulk property (which is minimized) during a molecular dynamics simulation. The simulation would start from some initial configuration and randomly distributed velocities for a initial parameterized potential. At fixed time intervals, the objective function would be computed and then the parameters of the potential updated according to some optimization routine (*e.g.*, simulated annealing). This procedure would then be iterated until the objective function is extremized.

An intriguing set of target materials are those that exhibit “inverse melting.”⁶⁶ Inverse melting is a first-order phase transition involving the crystal and liquid, but with a reversal from conventional melting in that addition of heat to the liquid, at constant pressure, causes that liquid to freeze into a crystalline solid. As a result of this reversal, the crystal has higher entropy than the isotropic liquid with which it coexists. This is a rare phenomenon, but real-world examples exist. For

example, the transition itself forms the basis of the zone-refining method for purification.¹²² Inverse melting has been studied as a “forward” problem using the Gaussian core potential model.⁶⁷ However, devising optimized interactions to make such unusual macroscopic behavior as robust as possible over a wide range of conditions has heretofore not been considered.

E. Toward Experimentally Realistic Interactions

An important component of future research should be the development of robust potentials (even if not optimal) for targeted structures and bulk properties that can be synthesized experimentally with colloids or other soft-matter systems. It is clear that there is wide class of target structures and bulk properties that can be achieved with pairwise additive potentials, both isotropic and anisotropic. In future research, it will be highly desirable to determine, when possible, the pair interactions that can be either be synthesized experimentally with colloids using current technology (*e.g.*, depletion, screening length, dipolar interactions, etc.) or can be done so in the near future. The latter could serve as a challenge to experimentalists.

Real interactions in many-particle materials at nondilute concentrations are necessarily nonadditive, *i.e.*, intrinsic three-body and higher-order interactions beyond pair interactions [explicitly given in Eq. (1)] are inevitable.^{89,104} Thus, it is crucial to determine how the effective pair potentials that result from the inverse approach correspond to the many-body interactions that arise in actual colloidal systems. This important problem has received little attention in the literature. It has been shown that effective pair interactions that approximate nonadditive potentials are in fact density dependent and hence one must be careful in carrying out the resulting statistical mechanics.⁸⁹ Guided by experiments, one can determine the real two-body and three-body interactions that together mimic the effective pair potential required to achieve the targeted many-particle configurations using both theoretical techniques and molecular dynamics simulations. This will require continual feedback between theory and experiment.

F. Incorporating Dynamics

The dominant theme of this review article concerned the determination of potentials that spontaneously create target structures under equilibrium or near-equilibrium circumstances. A conjugate kinetic problem also exists, in which selection among alternative irreversible scenarios (involving distinct dynamical evolutions) itself becomes a tool for selecting among alternative structural outcomes. The full potential of self-assembly to control and manipulate the structure of materials at the microscopic and nanoscopic level cannot be realized without

a deeper understanding of nonequilibrium processes at those length scales. For example, a recently developed model demonstrates this point by showing how the irreversible collisions in particle suspensions that generally produce diffusive chaotic dynamics can also cause the system to self-organize to avoid future collisions.¹²³ This can lead to a self-organized non-fluctuating quiescent state, with a dynamical phase transition separating it from fluctuating diffusing states. This investigation and many other nonequilibrium studies, too numerous to list here, provide exciting glimpses into the future of self-assembly. Inverse optimization techniques that exploit the dynamics of many-particle systems to achieve self-assembly has yet to be developed and should offer greater flexibility for novel material design.

G. Conclusions

Although in their infancy, the inverse approaches reviewed here have already shown a capability for controlling self-assembly to an exquisite degree. Indeed, future applications could revolutionize the manner in which materials are designed and fabricated, especially if there is continual feedback between theory and experiment. There are recent examples in which output from material optimization studies have been combined with experiments to produce novel materials or material components.^{124,125,126,127} These inverse methods have led to a deeper fundamental understanding of the mathematical relationship between the collective structural behavior of many-body systems and their interactions. For example, we have seen that low-coordinated crystal structures, chain-like arrays, and layered structures do not require directional interactions for self-assembly.^{18,19,20,22} Although soft matter with some of the interactions reviewed in this article cannot be synthesized with current technology, other optimized interactions described here that yield either novel structures or bulk properties are rather standard or could easily made in the laboratory^{20,23,26}. For practical purposes, it will be important that future research be directed toward producing optimized interactions with the constraint that they are experimentally achievable. We envision being able to “tailor” potentials that result in novel materials with varying degrees of disorder, thus extending the traditional idea of self-assembly to incorporate not only crystals but amorphous and quasicrystal structures.

Acknowledgments

This review article would not have been possible without my numerous collaborators. In particular, I am very grateful to Mikael Rechtsman, Obioma Uche and Robert Batten, who were instrumental in the interaction optimization work. I express special thanks to Frank Stillinger, who made major contributions to this research and was my co-author on a majority of the papers highlighted in this article. I am grateful to Antti-Pekka Hynninen for

supplying the image for Fig. 9. I thank the Institute for Advanced Study for its hospitality during his stay there. This work was supported by the Office of Basic Energy

Sciences, U.S. Department of Energy, under Grant DE-FG02-04-ER46108.

-
- * E-mail: torquato@princeton.edu
- ¹ G. M. Whitesides and P. E. Laibinis, *Langmuir*, 1990, **6**, 87–96.
 - ² S. A. Jenekhe and X. L. Chen, *Science*, 1999, **283**, 372–375.
 - ³ B. Grzybowski, A. Winkleman, J. A. Wiles, Y. Brumer, and G. M. Whitesides, *Nature Mater.*, 2003, **2**, 241–245.
 - ⁴ V. N. Manoharan, M. T. Elsesser, and D. J. Pine, *Science*, 2003, **301**, 483–487.
 - ⁵ A. M. Jackson, J. W. Myerson, and F. Stellacci, *Nature Mater.*, 2004, **3**, 330–336.
 - ⁶ M. P. Valignat, O. Theodoly, J. C. Crocker, W. B. Russel, and P. M. Chaikin, *Proc. Nat. Acad. Sci.*, 2005, **102**, 4225–4229.
 - ⁷ J. P. Hansen and I. R. McDonald, *Theory of Simple Liquids*, Academic Press, New York, 1986.
 - ⁸ M. P. Allen and D. J. Tildesley, *Computer Simulation of Liquids*, Oxford University Press, Oxford, England, 1987.
 - ⁹ D. Frenkel and B. Smit, *Understanding Molecular Simulation*, Academic Press, New York, 1996.
 - ¹⁰ C. N. Likos and H. Lowën, *Phys. Rev. Lett.*, 1999, **82**, 5289–5292.
 - ¹¹ A. Lang, C. N. Likos and H. Lowën, *J. Phys. Cond. Matter*, 2000, **12**, 5087–5108.
 - ¹² Z. Zhang and S. C. Glotzer, *Nano Lett.*, 2004, **4**, 1407–1413.
 - ¹³ G. Arya and A. Z. Panagiotopoulos, *Phys. Rev. E*, 2004, **70**, 031501:1–9.
 - ¹⁴ A.-P. Hynninen, C. G. Christova, R. van Roij, A. van Blaaderen, and M. Dijkstra, *Phys. Rev. Lett.*, 2006, **96**, 138308:1–4.
 - ¹⁵ M. A. Glaser, G. M. Grason, R. D. Kamien, A. Košmrlj, C. D. Santangelo, and P. Ziherl, *Europhys. Lett.*, 2007, **78**, 46004:1–5.
 - ¹⁶ E. Bianchi, P. Tartaglia, E. Zaccarelli, and F. Sciortino, *J. Chem. Phys.*, 2008, **128**, 144504:1–10.
 - ¹⁷ O. U. Uche, F. H. Stillinger, and S. Torquato, *Phys. Rev. E*, 2004, **70**, 046122:1–9.
 - ¹⁸ M. C. Rechtsman, F. H. Stillinger, and S. Torquato, *Phys. Rev. Lett.*, 2005, **95**, 228301:1–4; *ibid.*, 2006, **97**, 239901.
 - ¹⁹ M. C. Rechtsman, F. H. Stillinger, and S. Torquato, *Phys. Rev. E*, 2006, **73**, 011406:1–12; *ibid.*, 2007, **75**, 019902(E).
 - ²⁰ M. C. Rechtsman, F. H. Stillinger, and S. Torquato, *Phys. Rev. E*, 2006, **74**, 021404:1–7.
 - ²¹ O. U. Uche, S. Torquato, and F. H. Stillinger, *Phys. Rev. E*, 2006, **74**, 031104:1–10.
 - ²² M. Rechtsman, F. H. Stillinger, and S. Torquato, *Phys. Rev. E*, 2007, **75**, 031403.
 - ²³ M. C. Rechtsman, F. H. Stillinger, and S. Torquato, *J. Phys. Chem. A*, 2007, **111**, 12816–12821.
 - ²⁴ M. C. Rechtsman and S. Torquato, *J. Appl. Phys.*, 2008, **103**, 084901:1–15.
 - ²⁵ M. C. Rechtsman, H.-C. Jeong, P. M. Chaikin, S. Torquato, and P. J. Steinhardt, *Phys. Rev. Lett.*, 2008, **101**, 073902:1–4.
 - ²⁶ M. C. Rechtsman, F. H. Stillinger, and S. Torquato, *Phys. Rev. Lett.*, 2008, **101**, 085501:1–4.
 - ²⁷ R. D. Batten, F. H. Stillinger, and S. Torquato, *J. Appl. Phys.*, 2008, **104**, 033504:1–12.
 - ²⁸ F. H. Stillinger, S. Torquato, J. M. Eroles, and T. M. Truskett, *J. Phys. Chem. B*, 2001, **105**, 6592–6597.
 - ²⁹ H. Sakai, F. H. Stillinger, and S. Torquato, *J. Chem. Phys.*, 2002, **117**, 297–307.
 - ³⁰ S. Torquato and F. H. Stillinger, *J. Phys. Chem. B*, 2002, **106**, 8354–8359; *ibid.*, 2002, **106**, 11405.
 - ³¹ J. R. Crawford, S. Torquato, and F. H. Stillinger, *J. Chem. Phys.*, 2003, **119**, 7065–7074.
 - ³² F. H. Stillinger and S. Torquato, *J. Phys. Chem. B*, 2004, **108**, 19589–19594.
 - ³³ F. H. Stillinger and S. Torquato, *Mol. Phys.*, 2005, **103**, 2943–2949.
 - ³⁴ O. U. Uche, F. H. Stillinger, and S. Torquato, *Physica A*, 2006, **360**, 21–36.
 - ³⁵ S. Torquato and F. H. Stillinger, *Experimental Math.*, 2006, **15**, 307–331.
 - ³⁶ S. Torquato, O. U. Uche, and F. H. Stillinger, *Phys. Rev. E*, 2006, **74**, 061308:1–16.
 - ³⁷ A. Scardicchio, F. H. Stillinger, and S. Torquato, *J. Math. Phys.*, 2008, **49**, 043301:1–15.
 - ³⁸ W. B. Russel, D. A. Saville, and W. R. Schowalter, *Colloidal Dispersions*, Cambridge University Press, Cambridge, England, 1989.
 - ³⁹ C. A. Murray and D. G. Murray, *Ann. Rev. Phys. Chem.*, 1996, **47**, 421–462.
 - ⁴⁰ Z. Cheng, P. M. Chaikin, W. B. Russel, W. V. Meyer, J. Zhu, R. B. Rogers, and R. H. Ottewill, *Mater. & Design*, 2001, **22**, 529–534.
 - ⁴¹ M. E. Leunissen, A. van Blaaderen, A. D. Hollingsworth, M. T. Sullivan, and P. M. Chaikin, *Proc. Nat. Acad. Sci.*, 2007, **104**, 2585–2590.
 - ⁴² A. Yethiraj, *Soft Matter*, 2007, **3**, 1099–1115.
 - ⁴³ B. M. Mladek, D. Gottwald, G. Kahl, M. Neumann, and C. N. Likos, *Phys. Rev. Lett.*, 2006, **96**, 045701:1–4.
 - ⁴⁴ K. M. Ho, C. T. Chan, and C. M. Soukoulis, *Phys. Rev. Lett.*, 1990, **65**, 3152–3155.
 - ⁴⁵ C. Y. Kao, S. Osher, and E. Yablonovitch, *Appl. Phys. B - Lasers & Optics*, 2005, **B81**, 235–244.
 - ⁴⁶ O. Sigmund and K. Hougaard, *Phys. Rev. Lett.*, 2008, **100**, 153904:1–4.
 - ⁴⁷ W. Man, M. Megens, P. J. Steinhardt, and P. M. Chaikin, *Nature*, 2005, **436**, 993–996.
 - ⁴⁸ O. Sigmund and S. Torquato, *Appl. Phys. Lett.*, 1996, **69**, 3203–3205.
 - ⁴⁹ T. A. Mary, J. S. O. Evans, T. Vogt, and A. W. Sleight, *Science*, 1996, **272**, 90–92.
 - ⁵⁰ L. V. Gibiansky and S. Torquato, *J. Mech. Phys. Solids*, 1997, **45**, 1223–1252.
 - ⁵¹ R. Lakes, *Science*, 1987, **235**, 1038–1040.
 - ⁵² O. Sigmund, in *Proceedings of the third international conference on intelligent material, ICIM96, Lyon, June*, ed. P. Gobin, 1996. SPIE vol. 2779.
 - ⁵³ L. J. Gibson and M. F. Ashby, *Cellular Solids*, Cambridge

- University Press, Cambridge, England, second ed., 1997.
- ⁵⁴ G. W. Milton, *J. Mech. Phys. Solids*, 1992, **40**, 1105–1137.
 - ⁵⁵ G. Y. Wei and S. F. Edwards, *Phys. Rev. E*, 1998, **58**, 6173–6181.
 - ⁵⁶ B. Xu, F. Arias, S. T. Brittain, X.-M. Zhao, B. Gryzbowski, S. Torquato, and G. M. Whitesides, *Advanced Materials*, 1999, **11**, 1186–1189.
 - ⁵⁷ S. Torquato, L. V. Gibiansky, M. J. Silva, and L. J. Gibson, *Int. J. Mech. Sci.*, 1998, **40**, 71–82.
 - ⁵⁸ S. Torquato, *J. Mech. Phys. Solids*, 1998, **46**, 1411–1440.
 - ⁵⁹ S. Hyun and S. Torquato, *J. Mater. Res.*, 2001, **16**, 280–285.
 - ⁶⁰ S. Torquato, *Random Heterogeneous Materials: Microstructure and Macroscopic Properties*, Springer-Verlag, New York, 2002.
 - ⁶¹ S. Torquato, S. Hyun, and A. Donev, *Phys. Rev. Lett.*, 2002, **89**, 266601:1–4.
 - ⁶² S. Torquato and A. Donev, *Proc. R. Soc. Lond. A*, 2004, **460**, 1849–1856.
 - ⁶³ Y. Jung and S. Torquato, *Phys. Rev. E*, 2005, **92**, 255505:1–8.
 - ⁶⁴ G. Ferey and A. K. Cheetham, *Science*, 1999, **283**, 1125–1126.
 - ⁶⁵ B. Chen, M. Eddaoudi, S. T. Hyde, M. O’Keefe, and O. M. Yaghi, *Science*, 2001, **291**, 1021–1023.
 - ⁶⁶ A. L. Greer, *Nature*, 2000, **404**, 134–134.
 - ⁶⁷ M. R. Feeney, P. Debenedetti, and F. H. Stillinger, *J. Chem. Phys.*, 2003, **119**, 4582–4591.
 - ⁶⁸ D. A. Keen and R. L. McGreevy, *Nature*, 1990, **334**, 423–425.
 - ⁶⁹ A. P. Lyubartsev and A. Laaksonen, *Phys. Rev. E*, 1995, **52**, 3730–3737.
 - ⁷⁰ H. Meyer, O. Biermann, R. Faller, D. Reith, and F. Müller-Plathe, *J. Chem. Phys.*, 2000, **113**, 6264–6275.
 - ⁷¹ R. L. McGreevy, *J. Phys. Condens. Matter*, 2001, **13**, R877–R913.
 - ⁷² S. Torquato and F. H. Stillinger, *Phys. Rev. E*, 2003, **68**, 041113: 1–25.
 - ⁷³ J. Beck, *Acta Mathematica*, 1987, **159**, 1–49.
 - ⁷⁴ A. Gabrielli, B. Jancovici, M. Joyce, J. L. Lebowitz, L. Pietronero, and F. S. Labini, *Phys. Rev. D*, 2003, **67**, 043506:1–7.
 - ⁷⁵ A. Gabrielli and S. Torquato, *Phys. Rev. E*, 2004, **70**, 041105:1–12.
 - ⁷⁶ A. Gabrielli, M. Joyce, and S. Torquato, *Phys. Rev. E*, 2008, **77**, 031125:1–12.
 - ⁷⁷ A. Gabrielli, M. Joyce, and F. S. Labini, *Phys. Rev. D*, 2002, **65**, 083523:1–18.
 - ⁷⁸ P. J. E. Peebles, *Principles of Physical Cosmology*, Princeton University Press, Princeton, 1993.
 - ⁷⁹ R. P. Feynman and M. Cohen, *Phys. Rev.*, 1956, **102**, 1189–1204.
 - ⁸⁰ A. Donev, F. H. Stillinger, P. M. Chaikin, and S. Torquato, *Phys. Rev. Lett.*, 2004, **92**, 255506:1–4.
 - ⁸¹ R. P. Feynman, *Statistical Mechanics*, Westview Press, Boulder, Colorado, 1998.
 - ⁸² S. Torquato, A. Scardicchio, and C. E. Zachary, *J. Stat. Mech: Theory & Exp.*, 2008, in press.
 - ⁸³ G. E. Uhlenbeck in *Fundamentals of Statistical Mechanics*, ed. E. G. D. Cohen; Wiley, New York, 1968.
 - ⁸⁴ C. Radin, *Rev. Math. Phys.*, 1987, **3**, 125–135.
 - ⁸⁵ D. Gottwald, G. Kahl, and C. N. Likos, *J. Chem. Phys.*, 2005, **122**, 204503:1–11.
 - ⁸⁶ A. Sütő, *Phys. Rev. Lett.*, 2005, **95**, 265501:1–4.
 - ⁸⁷ A. Sütő, *Phys. Rev. E*, 2006, **74**, 104117:1–8.
 - ⁸⁸ S. Torquato and F. H. Stillinger, *Phys. Rev. Lett.*, 2008, **100**, 020602:1–4.
 - ⁸⁹ F. H. Stillinger, H. Sakai, and S. Torquato, *J. Chem. Phys.*, 2002, **117**, 288–296.
 - ⁹⁰ A.-P. Hynninen, T. Panagiotopoulos, M. C. Rechtsman, F. H. Stillinger, and S. Torquato, *J. Chem. Phys.*, 2006, **125**, 024505:1–5.
 - ⁹¹ J. Percus and G. Yevick, *Phys. Rev.*, 1958, **110**, 1–13.
 - ⁹² Y. Fan, J. K. Percus, D. K. Stillinger, and F. H. Stillinger, *Phys. Rev. A*, 1991, **44**, 2394–2402.
 - ⁹³ A. Donev, F. H. Stillinger, and S. Torquato, *Phys. Rev. Lett.*, 2005, **95**, 090604:1–4.
 - ⁹⁴ D. W. Schaefer, *Science*, 1989, **243**, 1023–1027.
 - ⁹⁵ C. J. Brinker and G. W. Scherer, *Sol-Gel Science: The Physics and Chemistry of Sol-Gel Processing*, Academic Press, New York, 1990.
 - ⁹⁶ A Bravais lattice is to be distinguished from the more general category of a *periodic structure* (i.e., crystal) in which the fundamental cell (still periodically replicated) contains one or more particles located anywhere in the cell. A periodic structure is sometimes referred to as a lattice with a *basis*.
 - ⁹⁷ C. E. Zachary, F. H. Stillinger, and S. Torquato, *J. Chem. Phys.*, 2008, **128**, 224505:1–16.
 - ⁹⁸ S. Torquato and F. H. Stillinger, to be published.
 - ⁹⁹ M. Yamada, *Prog. Theor. Phys.*, 1961, **25**, 579–594.
 - ¹⁰⁰ O. Costin and J. Lebowitz, *J. Phys. Chem. B.*, 2004, **108**, 19614–19618.
 - ¹⁰¹ T. Kuna, J. L. Lebowitz, and E. R. Speer, *J. Stat. Phys.*, 2007, **129**, 417–439.
 - ¹⁰² J. T. Chayes and L. Chayes, *J. Stat. Phys.*, 1984, **36**, 471–488.
 - ¹⁰³ P. G. Bolhuis, A. A. Louis, J. P. Hansen, and E. J. Meijer, *J. Chem. Phys.*, 2001, **114**, 4296–4311.
 - ¹⁰⁴ P. G. Bolhuis, A. A. Louis, and J. P. Hansen, *Phys. Rev. E*, 2001, **64**, 021801:1–12.
 - ¹⁰⁵ M. D. Rintoul and S. Torquato, *J. Colloid Interface Sci.*, 1997, **186**, 467–476.
 - ¹⁰⁶ C. L. Y. Yeong and S. Torquato, *Phys. Rev. E*, 1998, **57**, 495–506.
 - ¹⁰⁷ D. Cule and S. Torquato, *J. Appl. Phys.*, 1999, **86**, 3428–3437.
 - ¹⁰⁸ S. Torquato and F. H. Stillinger, *Phys. Rev. E*, 2006, **73**, 031106:1–8.
 - ¹⁰⁹ O. Sigmund and S. Torquato, *J. Mech. Phys. Solids*, 1997, **45**, 1037–1067.
 - ¹¹⁰ N. H. Fletcher, *The Chemical Physics of Ice*, Cambridge University Press, Cambridge University, 1970.
 - ¹¹¹ T. A. Mary, J. S. O. Evans, T. Vogt, and A. W. Sleight, *Science*, 1996, **272**, 90–92.
 - ¹¹² E. A. Jagla, *Phys. Rev. E*, 1998, **58**, 1478–1486.
 - ¹¹³ P. J. Camp, *Phys. Rev. E*, 2003, **68**, 061506:1–8.
 - ¹¹⁴ R. H. Baughman and D. S. Galvao, *Nature*, 1993, **365**, 735–737.
 - ¹¹⁵ R. H. Baughman, *Nature*, 2003, **425**, 667.
 - ¹¹⁶ L. V. Gibiansky and S. Torquato, *J. Mech. Phys. Solids*, 1997, **45**, 689–708.
 - ¹¹⁷ H. Carré and L. Daudeville, *J. Eng. Mech.*, 1999, **125**, 914–921.
 - ¹¹⁸ J. Zhang, H. Liu, Z. Wang and N. Ming, *J. Appl. Phys.*, **103**, 2008, 013517:1–4.
 - ¹¹⁹ Y. S. Cho, G. R. Yi, J. M. Lim, S. H. Kim, V. N. Manoharan, D. J. Pine, and S. M. Yang, *J. Am. Chem. Soc.*, 2005,

- 127**, 15968–15975.
- ¹²⁰ A. van Blaaderen, *Nature*, 2006, **439**, 545–546.
- ¹²¹ A. W. Wilber, J. P. K. Doye, A. A. Louis, E. G. Noya, M. A. Miller, and P. Wong, *J. Chem. Phys.*, 2007, **127**, 085106:1–12.
- ¹²² W. G. Pfann, *Zone Melting*, Wiley, New York, 1966.
- ¹²³ C. Laurent, P. M. Chaikin, J. P. Gollub, and D. J. Pine, *Nature Phys.*, 2008, **4**, 420–424.
- ¹²⁴ A. Donev, I. Cisse, D. Sachs, E. A. Variano, F. H. Stillinger, R. Connelly, S. Torquato, and P. M. Chaikin, *Science*, 2004, **303**, 990–993.
- ¹²⁵ W. Man, A. Donev, F. H. Stillinger, M. Sullivan, W. B. Russel, D. Heeger, S. Inati, S. Torquato, and P. M. Chaikin, *Phys. Rev. Lett.*, 2005, **94**, 198001:1–4.
- ¹²⁶ S. Torquato, A. Donev, A. G. Evans, and C. J. Brinker, *J. Appl. Phys.*, 2005, **97**, 124103:1–5.
- ¹²⁷ H. Fan, C. Hartshorn, T. Buchheit, D. Tallant, R. Sullivan, D. J. Lacks, S. Torquato, and C. J. Brinker, *Nature Mater.*, 2007, **6**, 418–423.